SA(IR)-244

UNITED STATES DEPARTMENT OF THE INTERIOR

GEOLOGICAL SURVEY

SAUDI ARABIAN PROJECT REPORT 244

ULTRAMAFIC INCLUSIONS AND HOST ALKALI OLIVINE BASALTS OF THE SOUTHERN COASTAL PLAIN OF THE RED SEA, KINGDOM OF SAUDI ARABIA

by

E. D. Ghent, R. G. Coleman, and D. G. Hadley

PREPARED FOR
DIRECTORATE GENERAL OF MINERAL RESOURCES
MINISTRY OF PETROLEUM AND MINERAL RESOURCES
JIDDAH, SAUDI ARABIA
1979

U.S. GEOLOGICAL SURVEY

SAUDI ARABIAN PROJECT REPORT 244

ULTRAMAFIC INCLUSIONS AND HOST ALKALI OLIVINE BASALTS OF THE SOUTHERN COASTAL PLAIN OF THE RED SEA, KINGDOM OF SAUDI ARABIA

by

E.D. Ghent, R.G. Coleman, and D.G. Hadley

U.S. Geological Survey
Jiddah, Saudi Arabia

1979

CONTENTS

ILLUSTRATIONS

TABLES

ULTRAMAFIC INCLUSIONS AND HOST ALKALI OLIVINE BASALTS OF THE SOUTHERN COASTAL PLAIN OF THE RED SEA, KINGDOM OF SAUDI ARABIA

by

E.D. Ghent[1/], R.G. Coleman[2/], and D.G. Hadley

ABSTRACT

A variety of mafic and ultramafic inclusions occur within the pyroclastic components of the Al Birk basalt, erupted on the southern Red Sea coastal plain of Saudi Arabia from Pleistocene time to the present. Depleted harzburgites are the only inclusions contained within the basalts that were erupted through Miocene oceanic crust (15 km thick) in the vicinity of Jizan, whereas to the north in the vicinity of Al Birk, alkali basalts that were erupted through a thicker Precambrian crust (48 km thick) contain mixtures of harzburgites, cumulate gabbro, and websterite inclusions accompanied by large (> 2 cm) megacrysts of glassy alumina-rich clinopyroxene, plagioclase, and spinel. Microprobe analyses of individual minerals from the harzburgites, websterites, and cumulate gabbros reveal variations in composition that can be related to a complex mantle history during the evolution of the alkali basalts. Clinopyroxene and plagioclase megacrysts may represent early phases that crystallized from the alkali olivine basalt magma at depths less than 35 km. Layered websterites and gabbros with cumulate plagioclase and clinopyroxene may represent continuing crystallization of the alkali olivine basalt magma in the lower crust when basaltic magma was not rapidly ascending. It is significant that the megacrysts and cumulate inclusions apparently form only where the magmas have traversed the Precambrian crust, whereas the harzburgite-bearing basalts that penetrated a much thinner Miocene oceanic crust reveal no evidence of mantle fractionation. These alkali olivine basalts and their contained inclusions are related in time to present-day rifting in the Red Sea axial trough. The onshore, deep-seated, undersaturated magmas are separated from the shallow Red Sea rift subalkaline basalts by only 170 km. The contemporaneity of alkaline olivine and subalkaline basalts requires that they must relate directly to the separation of the Arabian plate from the African plate.

1/ Department of Geology, University of Calgary, Calgary, Alberta, Canada.

2/ U.S. Geological Survey, Menlo Park, California.

INTRODUCTION

Work of the U.S. Geological Survey sponsored by the Ministry of Petroleum and Mineral Resources, Saudi Arabia, has revealed the presence of mafic and ultramafic inclusions within alkali olivine basalt (Hadley, 1975a, b) exposed along the narrow Red Sea coastal plain north of Jizan (fig. 1) as flows extruded from circular feeder pipes surrounded by small cinder cones. Geologic evidence and radiometric age determinations indicate that eruption of the alkali olivine basalt began in the Pleistocene and has continued to the present. All of the alkali olivine basalt erupted within this time span characteristically contains mafic and ultramafic inclusions. It is herein referred to as the Al Birk basalt (Coleman and others, 1977). The purpose of this paper is to describe the occurrence of the mafic and ultramafic inclusions and to document their mineralogy and chemistry as related to their host basalt.

Rifting of the Red Sea and formation of subalkaline basalts within the Red Sea axial trough some 170 km west of the coastal plain were contemporaneous with the formation of the Al Birk basalt (Coleman and others, 1977). As a consequence, contrasting magma types can be related to opening and sea-floor spreading of the Red Sea. Tertiary volcanic rocks are widespread within the Arabian Peninsula, particularly along its western border with the Red Sea. They are represented mainly by alkaline basalts that, together with those in Ethiopia and Yemen, make up one of the largest accumulations of undersaturated basaltic lavas in the world (Baker and others, 1972). These vast outpourings of plateau alkali basalts probably mark the beginning of the proto Red Sea and apparently continued to erupt as the thick Miocene evaporates and clastics were deposited in the Red Sea depression. To our knowledge, mafic or ultramafic inclusions have not been reported from these older and more widespread plateau basalts.

The present-day axial rift in the Red Sea began to develop sometime in the Pliocene ($\sim$ 5 m.y. ago) and was filled with subalkaline oceanic tholeiites (Ross and others, 1973). Contemporaneous with this axial rifting in the Red Sea are alkali olivine basalts of the Al Birk basalt that form small restricted flows on the southern Saudi Arabian coastal plain. North of the Ad Darb fault, the Al Birk basalt rests mainly on Precambrian crust that extends to the very edge of the Red Sea coastline. South of the Ad Darb fault, it rests partly on the Miocene oceanic crust formed during the initial opening of the Red Sea (Coleman and others, 1977) and partly on clastic sediments that onlap the Miocene oceanic crust. To avoid confusion in the discussion that follows, the Al Birk basalt resting on continental crust will be referred to as the northern volcanic field, and the basalt resting on Miocene oceanic crust and coastal plain deposits will be called the southern volcanic field. Ultramafic

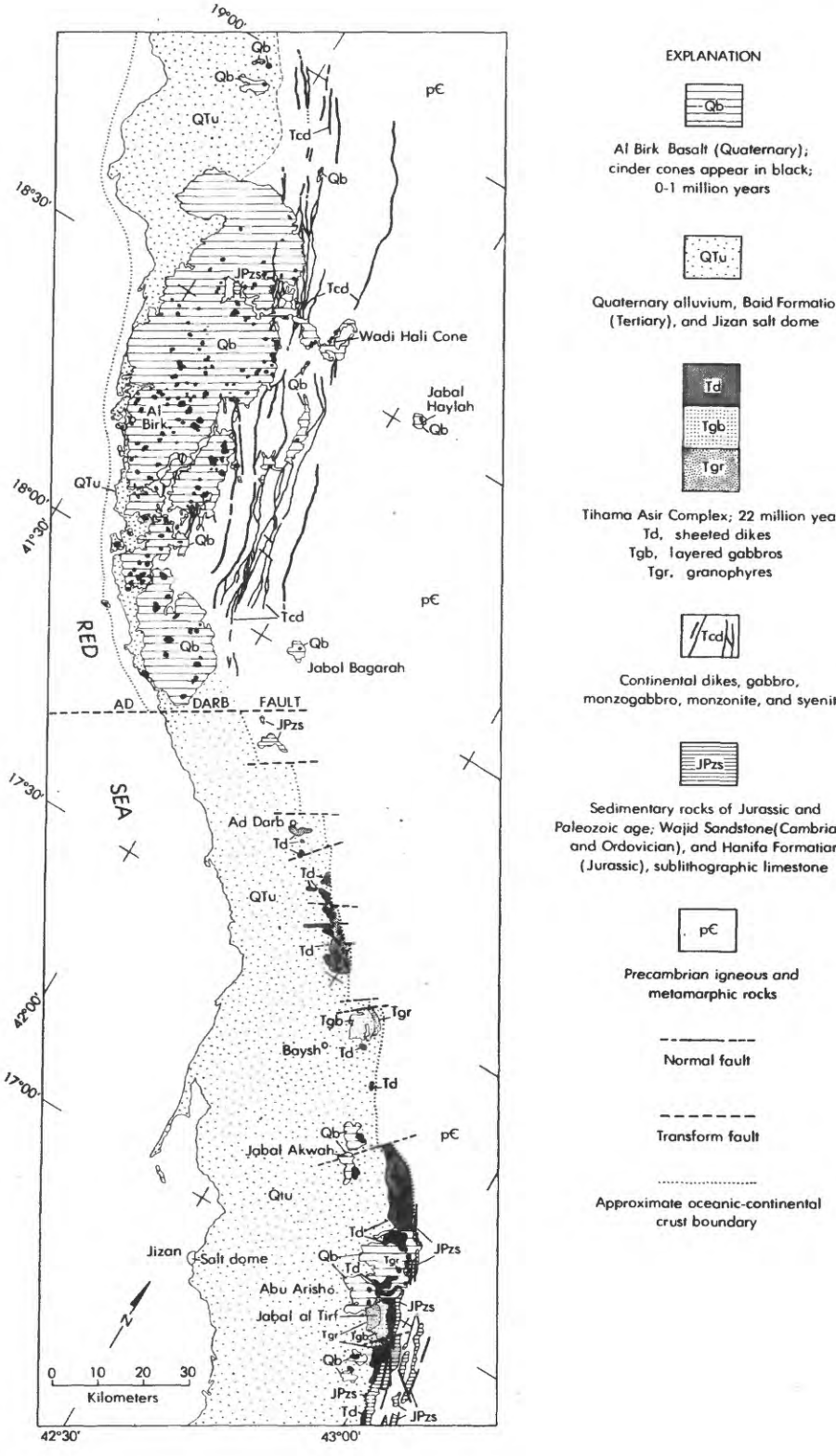

Figure 1. Simplified geologic map of southeastern coastal plain of the Red Sea, Saudi Arabia.

inclusions are most commonly found within the ejecta that form cinder cones around the feeder necks. It is significant that where the feeder necks and associated cinder cones penetrate the Miocene oceanic crust south of the Ad Darb fault, the inclusions are of harzburgites only; whereas north of the fault, where the feeder necks have presumably penetrated a thick Precambrian crust, the inclusions consist of mixtures of harzburgites, websterites, and cumulate gabbros. Gettings (1977) has estimated that the Precambrian crust in the Jabal al Tirf area is approximately 48 km thick and that the Miocene oceanic crust is only 15 km thick. Ultramafic inclusions have been reported from the widespread Pliocene to recent alkali olivine basalt flows found on the crest of the Yemen arch and in northwestern Saudi Arabia; there is no information regarding their mineralogical composition.

The cinder cones associated with the Al Birk basalt are deeply dissected. Reconstruction of their original shapes indicates that most of the cinder cones are less than 150 m in height with circular bases varying in diameter from 1 to 1.5 km. Several larger cones within the northern volcanic field attain heights of 300 m and basal diameters of 2.3 km. Flows associated with these cinder cones are fairly restricted, rarely extending more than 12 km from the central vent. Many of the cones were breached all the way to their bases by the outflowing lava. The larger ultramafic inclusions (> 10 cm) are restricted to the pyroclastic debris that makes up the cinder cones; smaller inclusions are present within the flow units themselves. In contrast to the earlier Miocene dike swarms that intrude the coastal plain rocks, all of the alkali olivine basalts extruded from central vents that have more or less circular feeder pipes. In the Jabal al Tirf area, where alkali olivine basalts invade Miocene oceanic crust, the area of extruded material is much less ($\sim$ 300 km^2) than that north of the Ad Darb fault where lava covers more than 2,000 km^2 (fig. 1).

We wish to thank the following people for critical reviews of the manuscript: E.W. Wolfe, M.H. Beeson, W.S. Baldridge, R. Batiza, A. Irving, J. Nicholls, and M.Z. Stout. Any remaining errors or murkiness are our responsibility. We particularly wish to thank Glenn Brown for his interest and help and for initially introducing us to these rocks.

Work on this paper was carried out in accordance with a work agreement between the U.S. Geological Survey and the Ministry of Petroleum and Mineral Resources, Kingdom of Saudi Arabia. Permission to publish these data is approved by the Deputy Minister, Directorate General for Mineral Resources, Saudi Arabia. Ghent acknowledges laboratory support from National Research Council of Canada Operating Grant A-4379.

INCLUSIONS

General description

Inclusions were collected from numerous cinder cones within the Al Birk basalt; those cinder cones containing visible inclusions or megacrysts are shown on the geologic map (fig. 1). A systematic population count of the inclusions from each of these localities was not possible under the field conditions in this area. Field observations and close examination of the inclusions returned for study suggest that there is a systematic difference between the inclusion assemblages from the northern and southern volcanic fields. The inclusions from the southern volcanic field are of harzburgites only (fig. 2). Here the volcanic feeders have penetrated only oceanic crust formed during Miocene time (Coleman and others, 1977), and the inclusions are nearly always present within the lavas. Extended search within the pyroclastic debris produced no inclusions. Inclusions found in lavas are elongate spheroids ranging in size from 2 to 5 cm. Nearly all specimens are extremely friable and granulate easily. The high magnesium content of some lavas can be explained by contamination resulting from the break-up of these inclusions during eruption, resulting in wide dispersal of xenocrystic olivine and orthopyroxene.

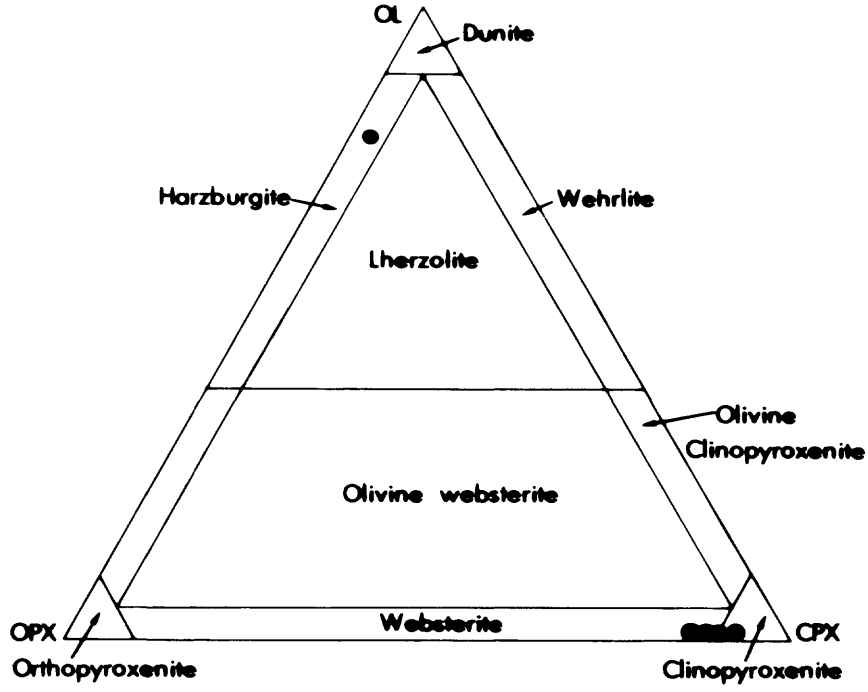

Figure 2. Ternary diagram with end members orthopyroxene, clinopyroxene, and olivine showing modal compositions of ultramafic inclusions from southern coastal plain of the Red Sea, Saudi Arabia.

In the northern volcanic field, where lavas were supplied by feeder pipes that came through Precambrian crust, the inclusion population is much more variable. Boulder-size inclusions, 4 to 20 cm in size, are present in the tephra as well as in some flows near the feeder necks or dikes. Xenocrystic olivine is present in many of the lavas, accompanied by orthopyroxene and a bright-green clinopyroxene. In some cones, websterites (fig. 2) and layered gabbros are much more abundant than the harzburgites. Large megacrysts (to 5 cm) of glassy black clinopyroxene are abundant only in those vents that contained websterite inclusions. Rare plagioclase megacrysts were found associated with the clinopyroxene megacrysts.

Ultramafic inclusions

Petrography

Harzburgites.--Harzburgite inclusions are composed of a mosaic of subhedral to anhedral olivine, generally 2 to 4 mm in diameter, and orthopyroxene, with minor chromium-spinel and green clinopyroxene (table 1, figs. 2, 3). Even where olivine shows crystal faces, these interlock perfectly with adjacent anhedral grains (fig. 3). Smaller anhedral to subhedral olivine grains occur adjacent to larger grains of olivine and pyroxene and generally have smooth, regular boundaries with olivine and pyroxene. About half of the larger olivine grains are cut by strain bands subparallel to {100} that generally divide single grains into two or three zones having different optical orientations (compare Talbot and others, 1963, p. 164). Trains of fluid inclusions are present in most of the olivine grains. Orthopyroxene shows a range of grain sizes; the larger orthopyroxenes are generally suggestive of grain-boundary equilibrium; that is, grain-boundary angles typically approach 120°. In some samples, orthopyroxene grains are molded against olivine; at other places, orthopyroxene partly encloses olivine. Clinopyroxene is anhedral and occurs molded against longer grains of olivine and orthopyroxene. Lamellar structure was rarely observed in orthopyroxene and clinopyroxene. Brown chromium-spinel occurs as irregular-shaped grains interstitial to olivine and orthopyroxene.

At the contact between inclusions and the enclosing basalt, olivine and orthopyroxene grains are corroded and invaded by dusty fine-grained basalt. Locally olivine is partly recrystallized to equigranular aggregates of grains about 0.1 mm in diameter. Xenocrysts of olivine are concentrated in the basaltic matrix adjacent to the inclusions (for example, JT-26).

Table 1.--*Modal analyses of ultramafic inclusions in basalts, coastal plain, Saudi Arabia*

Mineral	JT-26	58376A	58376C	58376D	58376E
Orthopyroxene	16.9	10.9	1.0	16.8	17.2
Clinopyroxene	1.4	88.1	56.9	81	79.4
Olivine	79.6	----	----	----	----
Spinel	.9	.95	27.9	2.2	3.2
Plagioclase	----	----	9.4	----	----

Sample localities, figure 1

JT-26, Harzburgite, Jibal Akwah
58376A, Websterite, Jabal Haylah
58376C, Spinel clinopyroxenite, Jabal Haylah
58376D, Websterite, Jabal Haylah
58376E, Websterite, Jabal Haylah

Clinopyroxenite-websterite.--Clinopyroxenite-websterite inclusions are largely composed of very light green clinopyroxene with minor pink orthopyroxene plus or minus green spinel. The clinopyroxene and orthopyroxene show a polygonal mosaic of grains that interlock perfectly. Even where there is a large difference in grain size, adjacent grains showed grain-boundary angles approaching 120° and suggest grain-boundary equilibrium (fig. 4).

Clinopyroxene grains are as much as 4 mm in maximum dimension, but in some samples (58376C), grains 0.5 mm in diameter are not uncommon. Larger clinopyroxene grains show undulatory extinction in polygonal sectors. Other grains show lamellar structure (twinning) parallel to {100}. Some grains (58376B) have border zones approximately 0.2 mm wide that show a spongy texture characterized by opaque inclusions (near 0.02 mm in diameter). Clinopyroxene in these border zones is in optical continuity with the inclusion-free central parts of the grains and shows no difference in chemical composition. In some samples (58376C), finer grained clinopyroxene is intergrown with spinel in a texture resembling that in gabbro inclusions (described later).

Orthopyroxene is typically in the 0.2-0.5 mm range, but some grains are as much as 3 mm in maximum dimension. Smaller equant grains of orthopyroxene occur interstitial to, and included within, larger clinopyroxene grains. The orthopyroxenes typically have rounded outlines, but some grains show crystal faces. In sample 58376C, fine-grained orthopyroxene is intergrown with spinel in a texture resembling the "reaction texture" in gabbros (see later section).

Large grains of spinel occur in clusters as much as 4 mm or more in diameter and as scattered grains (0.2 mm diameter in the groundmass). (See, for example, Nielson-Pike and Schwarzman, 1977, p. 56.) Most of the spinel is partly altered to reddish-brown limonitic material.

Associated with spinel (58376C) is a phase that is light brown to gray and composed of very fine-grained fibrous aggregates showing very low birefringence and choked with dusty opaque material. Qualitative microprobe analysis indicates the presence of silicon, aluminum, calcium, and iron. The grain shapes and alteration products suggest that the phase is highly altered plagioclase.

Chemistry

Major-oxide and trace-element analyses and CIPW normative values for ultramafic inclusions from Jabal Akwah within the southern volcanic field and from Jabal Haylah within the northern volcanic field are presented in table 2. The analytical data for harzburgite from Jabal Akwah suggest that partial melting of such rocks cannot account for the basaltic lavas with which they are associated, as the harzburgites are extremely depleted in aluminum, calcium, titanium, sodium, potassium, strontium, phosphorous, and lanthanum and enriched in nickel and chromium relative to the basalts (tables 2 and 11). Our interpretation is that these harzburgites must represent refractory mantle material from which magma has been previously extracted.

Websterites and clinopyroxenite from Jabal Haylah are similar in major-element chemistry to xenoliths of the aluminum-pyroxene-rich suite from Australia (Irving, 1974a), Kod Ali Island, southern Red Sea (Hutchison and Gass, 1971), and other places. A number of workers (for example, White, 1966; Green and Ringwood, 1967a; Irving, 1974a) have suggested that many such pyroxene-rich xenoliths represent accumulates crystallized at high pressure from basaltic magmas. This hypothesis is examined in more detail in the following sections.

Mineralogy

Olivine from harzburgite has a composition of Fo_{91} (table 3) and is homogeneous on the scale of a few microns. The composition of these olivines is comparable to that in other olivine-rich ultramafic inclusions (for example, Ross and others, 1954).

Spinels from harzburgites are rich in chromium whereas those from clinopyroxenites are relatively poor in chromium (table 4). Chromium-rich spinels are characteristic of many

Table 2.--*Chemical, normative, and spectrographic analyses of ultramafic inclusions in basalts, coastal plain, Saudi Arabia*

[Chemical analyses by rapid-rock methods described in USGS Bull. 1144A. Analysts, P.L.D. Elmore, Hezekiah Smith, James Kelsey, and J.L. Glenn. Spectrographic analyses supplemented by atomic absorption. Analyst, R.E. May.]

	Harzburgite		Websterite		
Sample No.	JT-26A	JT-26B	58376A	58376B	58377
	Chemical analyses (in weight percent)				
SiO_2	44.5	44.8	50.8	51.2	51.3
Al_2O_3	.80	2.0	7.3	6.2	5.4
Fe_2O_3	.54	.43	1.5	2.4	3.4
FeO	7.6	7.7	4.4	6.5	5.3
MgO	45.2	43.3	17.5	19.2	18.1
CaO	.80	1.0	16.4	12.1	14.5
Na_2O	.04	.17	.89	1.0	.73
K_2O	.07	.04	.05	.00	.04
H_2O^+	.32	.38	.40	.46	.39
H_2O^-	.96	.03	.05	.10	.07
TiO_2	.04	.05	.54	.63	.53
P_2O_5	.04	.05	.02	.05	.04
MnO	.07	.06	.08	.14	.12
CO_2	<.05	<.05	<.05	<.05	<.05
Sum	100.98	100.01	99.93	99.98	99.92
	CIPW norms (in molecular percent)				
or	0.41	0.24	0.30	0.00	0.24
ab	.34	1.44	7.54	8.46	6.18
an	1.80	4.58	15.79	12.43	11.35
wo	.80	.02	27.35	19.74	25.21
en	18.45	19.04	30.38	39.11	42.51
fs	2.22	2.44	4.25	7.50	5.91
fo	65.88	62.22	9.28	6.11	1.83
fa	8.76	8.78	1.43	1.29	.28
mt	.78	.62	2.18	3.48	4.93
il	.00	.10	1.03	1.20	1.01
ap	.10	.12	.05	.12	.10
di	1.50	.046	51.70	37.49	47.66
hy	19.97	21.46	10.28	28.86	25.98
ol	74.64	71.00	10.71	7.40	2.11
	Semiquantitative spectrographic analyses (in parts per million)				
Ba	1.5	1.5	N	2	2
Co	150	150	50	50	50
Cr	2000	2000	1500	2000	1500
Cu	1.5	1.5	50	150	70
Ni	3000	2000	500	500	300
Sc	10	10	70	70	100
Sn	20	20	15	20	15
Sr	N	N	50	100	70
V	30	20	500	300	500
Y	N	N	10	10	10
Ga	N	N	7	7	7
Yb	N	N	2	2	2

For sample localities, see table 1, figure 1.

Table 3.--*Electron microprobe analyses of olivines from ultramafic inclusions and basalts, coastal plain, Saudi Arabia*

[gr = groundmass of basalt enclosing nodule; core = core of olivine phenocrysts in basalt enclosing nodule; rim = rim of olivine phenocrysts in basalt enclosing nodule; ph = phenocrysts of basalt]

		Basalt							
Sample No.	Inclusion JT-26A**	JT-26A core	JT-26A rim	JT-26 gr	58375 ph gr	58377 ph gr	58378 ph gr	58524 ph gr	JT-26 ph gr
SiO_2	40.7	40.6	39.2	38.6	39.5	37.7	39.1	39.4	38.9
FeO*	9.1	9.0	17.0	18.9	13.1	26.7	15.1	14.2	14.4
NiO	.46	----	----	----	----	----	----	----	----
MnO	.1	----	----	----	----	----	----	----	----
MgO	49.7	49.4	43.4	41.7	45.7	35.2	44.9	44.9	44.4
CaO	.1	----	----	----	.3	.4	.25	.3	.3
Sum	100.2	99.0	99.6	99.2	98.6	100.0	99.3	98.8	98.0
		Number of ions on the basis of 4 oxygens							
Si	0.99	1.00	1.00	1.00	1.00	1.00	0.99	1.00	1.00
Fe	.19	.19	.36	.41	.28	.59	.32	.30	.31
Ni	.01	----	----	----	----	----	----	----	----
Mn	.00	----	----	----	----	----	----	----	----
Mg	1.81	1.81	1.64	1.60	1.72	1.39	1.69	1.70	1.69
Ca	.00	----	----	----	.01	.00	.01	.01	.01
Sum of Vi cations	2.01	2.00	2.00	2.01	2.01	1.98	2.02	2.01	2.01
		End member and ion proportions							
X_{Fe}/X_{Mg}	0.10	0.10	0.22	0.26	0.16	0.42	0.19	0.18	0.18
Fe_2SiO_4	9	9	18	20	14	30	16	15	16
Ni_2SiO_4	0	----	----	----	----	----	----	----	----
Mg_2SiO_4	91	91	82	80	86	70	84	85	84
Range in Fo	----	----	----	----	81-87	67-88	79-88	77-88	78-90

* denotes total Fe as FeO

** JT-26A and JT-26B olivine have analyses that are identical within analytical error

Table 4.--*Electron microprobe analyses of spinels from ultramafic inclusions and spinel megacrysts, coastal plain, Saudi Arabia*

	Harzburgite JT-26B	Websterite 58376C	Megacryst 93398A	
Chemical analyses (in weight percent)			Electron microprobe	Wet chemical
SiO_2	<0.05	0.05	0.03	0.62
Cr_2O_3	34.14	.86	.03	.02
Al_2O_3	32.70	64.65	54.82	53.22
Fe_2O_3[1/]	4.49	2.36	11.76	11.02
FeO	10.29	13.44	18.82	17.28
MgO	17.43	18.89	15.40	15.32
TiO_2	.2	.1	1.25	1.21
MnO	.2	.1	----	.15
Sum	99.45	100.4	102.11	98.84
Number of ions on basis of 4 oxygens and cations normalized to 3				
Cr	0.78	0.02	0.00	
Al	1.12	1.93	1.71	
Fe^{+3}	.10	.04	.23	
Fe^{+2}	.25	.28	.42	
Mg	.75	.71	.61	
Ti	.00	.00	.02	
Semiquantitative spectrographic analysis (in parts per million)				
Co			60	
Cr			26	
Cu			6	
Ni			55	
Sc			< 4	
V			150	
Y			<20	
Zr			<20	

1/ Fe_2O_3 and FeO contents estimated from total analyses using total cations = 3 and the following two equations in two unknowns: (1) 2 x number of moles of Fe^{+2} + 3 x number of moles of Fe^{+3} + sum of all other cationic changes = 8; (2) number of moles of Fe^{+2} = number of moles of Fe^{+3} = total number of moles of Fe.

Sample localities, figure 1

Table 5.--*Electron microprobe analyses of orthopyroxenes from ultramafic nodules, coastal plain, Saudi Arabia*

	Harzburgite		Websterite		
Sample No.	JT-26A	JT-26B	58376A	58376B	58376C
	Chemical analyses (in weight percent)				
SiO_2	55.8	55.3	53.3	52.6	53.2
TiO_2	.03	.06	.1	.2	.2
Al_2O_3	2.5	3.1	5.9	4.3	6.7
Cr_2O_3	.6	.7	.1	.3	<.02
FeO[a]	5.8	5.8	10.0	12.4	10.6
MnO	.1	.1	.2	.2	.2
MgO	34.6	34.1	30.5	29.0	29.4
CaO	.9	1.1	.7	.9	1.1
Na_2O	.03	.05	.06	.1	.07
Sum	100.4	100.3	100.9	100.0	101.5
	Number of ions on the basis of 6 oxygens				
Si	1.92	1.91	1.86	1.88	1.85
Al IV	.08	.09	.14	.12	.15
Sum	2.00	2.00	2.00	2.00	2.00
Al VI	0.02	0.03	0.10	0.06	0.12
Ti	0.00	0.00	0.00	0.01	0.01
Cr	.02	.02	.00	.01	.00
Fe	.17	.17	.29	.37	.31
Mn	.00	.00	.01	.01	.01
Mg	1.78	1.75	1.58	1.54	1.52
Ca	.03	.04	.03	.03	.04
Na	.00	.00	.00	.01	.00
Sum	2.02	2.01	2.01	2.04	2.01
	Proportions of ions				
X_{Fe}/X_{Mg}	0.10	0.10	0.18	0.24	0.20

a--total Fe calculated as FeO
For sample localities, see table 1

Table 6.--*Electron microprobe analyses of clinopyroxenes from mafic and ultramafic inclusions, alkali olivine basalts, and clinopyroxene megacrysts, coastal plain, Saudi Arabia*

	Harzburgite		Websterite			Basalt	Websterite		Megacrysts	
Sample No.	JT-26A	JT-26B	58376A	58376B	58376C	58377B	58377X	58377M	98398aM	98298bM
					(in weight percent)					
SiO_2	53.1	52.5	50.8	50.2	52.6	49.0	51.9	51.9	47.8	47.4
TiO_2	.09	.2	.6	.8	.8	1.9	.5	.5	1.7	1.7
Al_2O_3	2.9	3.6	7.0	6.4	7.4	4.1	5.3	5.3	9.0	9.2
Cr_2O_3	1.1	1.3	.2	.6	.06	----	.9	.9	<.03	<.03
Fe_2O_3 [1]	----	----[2]	1.2	1.7	1.4	----[2]	----	----[2]	----	----
FeO	2.5[2]	2.9[2]	3.4	4.9	3.9	7.9[2]	4.0	4.0[2]	7.1	6.8
MnO	.07	.07	.1	.1	.1	----	.1	.1	.1	.1
MgO	17.6	17.3	14.5	14.1	14.6	13.4	15.2	15.2	13.6	13.7
CaO	22.7	21.2	22.0	19.7	20.3	21.9	21.2	21.2	19.8	20.1
Na_2O	.4	.6	.7	1.1	.8	.6	1.1	1.1	1.0	1.0
Sum	100.5	99.7	100.5	99.6	102.0	99.2	100.2	100.2	100.1	100.0
					Number of ions on the basis of 6 oxygens					
Si	1.92	1.91	1.84	1.85	1.87	1.85	1.89	1.89	1.77	1.75
Al IV	.08	.09	.16	.15	.13	.15	.11	.11	.23	.25
Sum of IV cations	2.00	2.00	2.00	2.00	2.00	2.00	2.00	2.00	2.00	2.00
Al	0.04	0.07	0.14	0.13	0.18	0.03	0.11	0.11	0.16	0.15
Ti	.00	.01	.02	.02	.02	.05	.01	.01	.05	.05
Cr	.03	.04	.01	.02	.00	----	.03	.03	.00	.00
Fe^3	----	----	.03	.05	.04	----	----	----	----	----
Fe^2	.08	.09	.10	.15	.12	.25	.12	.12	.22	.21
Mn	.00	.00	.00	.00	.00	----	.00	.00	.00	.00
Mg	.95	.94	.78	.77	.77	.76	.83	.83	.74	.75
Ca	.88	.83	.86	.78	.77	.89	.83	.83	.78	.80
Na	.03	.04	.05	.08	.06	.04	.08	.08	.07	.07
Sum of cations	2.01	2.02	1.99	2.00	1.96	2.02	2.01	2.01	2.03	2.03

[1] Fe^2/Fe^3 calculated for pyroxene by assuming same Fe^2/Fe^3 as bulk rock analyses.

[2] Total Fe as FeO.

Table 7.--*Minor-element abundances in clinopyroxene megacrysts and clinopyroxenes from ultramafic inclusions, coastal plain, Saudi Arabia*

[TiO_2 in weight percent; all other analyses in parts per million (ppm). Quantitative spectrographic analyses considered accurate to ±15 percent except near limit of detection. Analyses 1-3 by R.E. Mays, 4-6 by Chris Heropoulos]

	1	2	3	4	5	6
		Megacrysts		Harzburgite		Websterite
Sample No.	98398-aM	98398-bM	983-98-B-3	JT-26A	JT-26B	58377
TiO_2	0.14	1.55	0.63	0.22	0.12	0.67
Mn	n.d.	n.d.	n.d.	740	1250	940
Ba	n.d.	n.d.	n.d.	<4	4	<4
Co	70	40	40	34	80	39
Cr	1300	500	12800	7300	5700	8700
Cu	8	55	8	11	8	80
Ni	300	150	460	410	750	480
Sc	70	70	60	75	28	57
Sr	n.d.	n.d.	n.d.	70	<10	52
V	150	460	360	290	115	290
Y	<20	30	<20	<15	<15	26
Zr	<20	50	<20	24	8	28
Ga	n.d.	n.d.	n.d.	<4	<4	9
Yb	n.d.	n.d.	n.d.	<1	<1	1

Table 8.--*Chemical, normative, and spectrographic analyses of gabbro inclusions, basalts, coastal plain, Saudi Arabia*

[Chemical analyses by rapid-rock methods. Rapid-rock analyses by Lowell Artis, by methods described under "Single Solution" in USGS Bulletin 1401; quantitative spectrographic analyses by Chris Heropoulos]

	Gabbro		
Sample No.	93413 A	93413 B	93413 C
Chemical analyses (in weight percent)			
SiO_2	45.7	44.4	44.9
Al_2O_3	17.0	16.8	17.5
Fe_2O_3	5.7	8.3	6.2
FeO	4.8	6.2	5.1
MgO	13.0	8.3	13.8
CaO	10.6	12.1	9.2
Na_2O	1.5	1.1	1.4
K_2O	.04	.00	.11
H_2O+	.27	.26	.40
H_2O-	.08	.08	.15
TiO_2	.56	.64	.47
P_2O_5	.06	.06	.07
MnO	.11	.21	.00
CO_2	.05	.04	.00
	99.47	98.49	99.30
CIPW norms (in molecular percent)			
Q	.00	2.13	.00
Or	.24	.00	.65
Ab	13.42	10.27	12.55
An	39.40	42.53	41.08
Di	9.84	15.37	3.23
Hy	19.52	19.52	22.86
Ol	10.63	.00	12.36
Mt	5.94	9.02	6.47
Il	.78	.03	.65
AP	.12	.13	.15
Cc	.13	.00	.00
Quantitative spectrographic analysis (in parts per million)			
Co	84	61	85
Cr	330	68	330
Cu	71	75	76
Ni	240	71	230
Sc	50	81	47
V	330	500	250
Y	<10	71	<10
Zr	<15	<15	<15

Table 9.--*Representative electron microprobe analyses of coexisting clinopyroxenes and orthopyroxenes from gabbro inclusions, coastal plain, Saudi Arabia*

[cc = clinopyroxene cores; cr = clinopyroxene rims; oc = orthopyroxene cores; or = orthopyroxene in "reaction fabric"]

	98413A			
Sample no.	(cc)	(cr)	(oc)	(or)
	Chemical analyses (in weight percent)			
SiO_2	49.1	48.1	50.1	50.2
TiO_2	1.0	1.0	.3	.3
Al_2O_3	8.2	9.7	7.0	7.3
Cr_2O_3	.1	.1	----	----
FeO	8.6	8.6	15.8	15.5
MgO	13.0	13.0	25.2	24.9
CaO	18.5	18.5	1.4	1.3
Na_2O	1.0	1.1	.1	.1
Sum	99.5	100.1	99.9	99.6
	Number of ions on the basis of 6 oxygens			
Si	1.82	1.78	1.82	1.82
Al IV	.18	.22	.18	.18
Sum of IV cations	2.00	2.00	2.00	2.00
Al VI	0.18	0.20	0.12	0.13
Ti	.03	.03	.01	.01
Cr	.00	.00	----	----
Fe	.27	.27	.48	.47
Mg	.72	.73	1.36	1.35
Ca	.74	.73	.05	.05
Na	.07	.08	.01	.01
Sum of VI cations	2.01	2.04	2.03	2.02

Table 10.--*Electron microprobe analyses of plagioclase from alkali olivine basalts, mafic and ultramafic inclusions, and megacrysts, coastal plain, Saudi Arabia*

[Analyses in molecular percent. An = anorthite; Or = orthoclase]

Sample no.	Anorthite	Orthoclase	Range of An in sample
1. JT-26	65	1.7	59-68
2. 58375	60	1.6	50-64
3. 58377	62	1.6	49-68
4. 58378	60	1.7	45-68
5. 58376C	55	2.5	49-58
6. 93410	54	.1	
7. 93413A	55	1.0	51-60
8. 93413A	54	1.0	51-56
9. 93413A	54	.9	53-55
10. 93398	44	2.5	
11. 93415	44	2.5	
12. 93415	60	2	50-71

1-4. Groundmass plagioclase from basalts.

5. Fine-grained plagioclase in contact with spinel and altered plagioclase(?) in ultramafic inclusion.

6,8. Granoblastic plagioclase from "reaction fabric" in gabbro inclusions.

7. Cumulus plagioclase in gabbro inclusion.

9. Plagioclase included in clinopyroxene.

10,11. Plagioclase megacrysts.

12. Groundmass plagioclase adjacent to plagioclase megacryst.

Table 11.--*Chemical, normative, and semiquantitative spectrographic analyses of host alkali olivine basalts, coastal plain, Saudi Arabia*

[Rapid rock analyses, P.L.D. Elmore, Hezekiah Smith, James Kelsey, J.L. Glenn. Chemical analyses by rapid-rock methods described in USGS Bulletin 1144A, supplemented by atomic absorption; semiquantitative spectrographic analyses analyst, Chris Heropoulos.]

	Harzburgite inclusions	Clinopyroxenite inclusions		
	Jabal Akwah	Jabal Haylah		
Sample no.	JT-26	58375	58377	58378
	Chemical analyses (in weight percent)			
SiO_2	43.8	47.3	46.5	46.6
Al_2O_3	14.0	14.8	15.4	16.2
Fe_2O_3	2.2	2.1	3.5	3.4
FeO	7.0	8.9	8.0	7.7
MgO	11.8	9.5	8.8	7.6
CaO	10.0	9.0	9.5	9.7
Na_2O	1.8	3.5	3.3	3.0
K_2O	1.1	1.2	1.1	1.1
H_2O^+	3.3	.69	.72	1.1
H_2O^-	1.4	.12	.12	.35
TiO_2	2.2	1.7	2.0	2.2
P_2O_5	.63	.60	.53	.53
MnO	.17	.19	.22	.23
CO_2	.09	<.05	<.05	.11
Sum	99.49	99.60	99.69	99.82
Specific gravity powder	2.92	3.00	3.00	3.00
	CIPW norms (in molecular weight percent)			
Or	6.53	7.12	6.52	6.51
Ab	15.31	23.22	23.14	25.43
An	27.01	21.21	24.03	27.54
Ne	.00	3.53	2.63	.00
Wo	7.58	8.22	8.26	6.89
En	8.57	5.11	5.45	5.03
Fs	2.25	2.62	2.21	2.16
Fo	14.69	13.07	11.59	9.76
Fa	4.25	7.40	5.19	4.62
Mt	3.21	3.06	5.09	4.94
Il	4.20	3.24	3.81	4.19
Ap	1.50	1.43	1.26	1.26
Cc	.21	.00	.00	.25
Di	14.47	15.95	15.92	13.31
Hy	3.93	.00	.00	.78
Ol	18.94	20.47	16.78	14.38
Pl (an + ab)	42.32	44.44	47.17	52.97
	Semiquantitative spectrographic analyses (in parts per million)			
Ba	500	300	200	300
Co	30	30	50	30
Cr	700	1000	500	300
Cu	50	70	70	70
La	100	50	50	50
Nb	70	30	30	30
Ni	500	300	200	200
Sc	30	50	50	50
Sr	1000	1000	1000	1000
V	200	150	200	200
Y	50	30	30	50
Zr	200	150	150	150

olivine-rich ultramafic xenoliths; chromium-poor spinels are found in xenoliths rich in aluminous pyroxenes (see, for example, Irving, 1974a).

Orthopyroxenes and clinopyroxenes from harzburgites have a higher Mg/Fe ratio, a higher chromium content, and a lower aluminum content than those from websterites and clinopyroxenites (tables 5 and 6). In addition, clinopyroxenes from websterites and clinopyroxenites are rich in sodium and titanium relative to those of harzburgites (tables 6 and 7).

Clinopyroxene analyses for websterite and clinopyroxenite have been recalculated, assuming that they have the same ferrous-ferric ratio as the bulk rock of which they are the major iron-bearing phase (tables 1, 2, and 6).

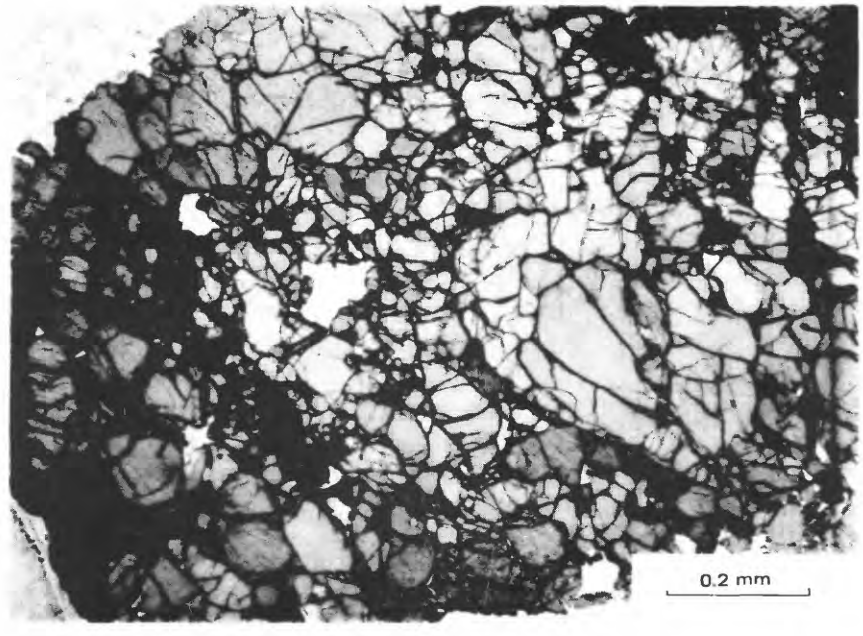

Figure 3. Photomicrograph of harzburgite showing textures of grain boundary equilibrium.

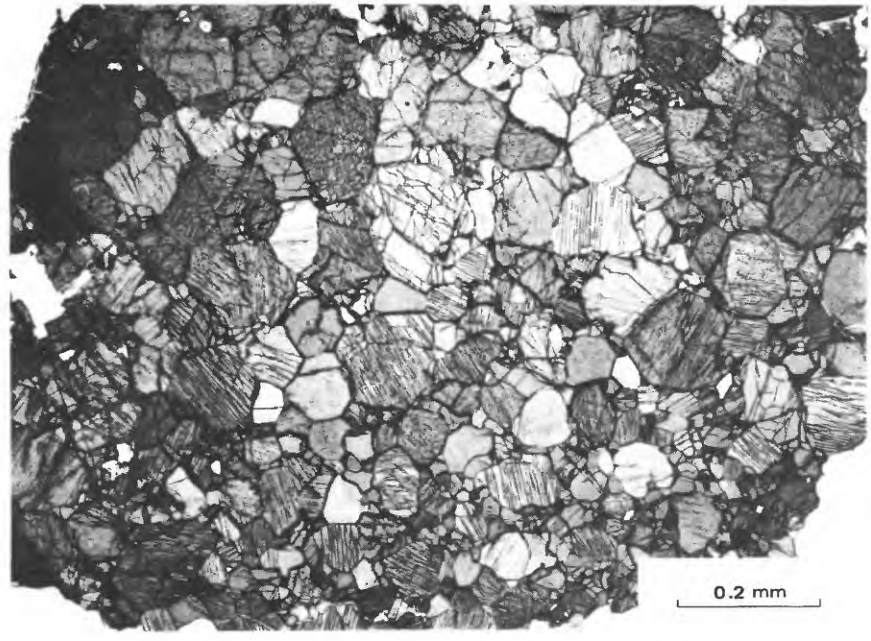

Figure 4. Photomicrograph of websterite showing textures of grain boundary equilibrium.

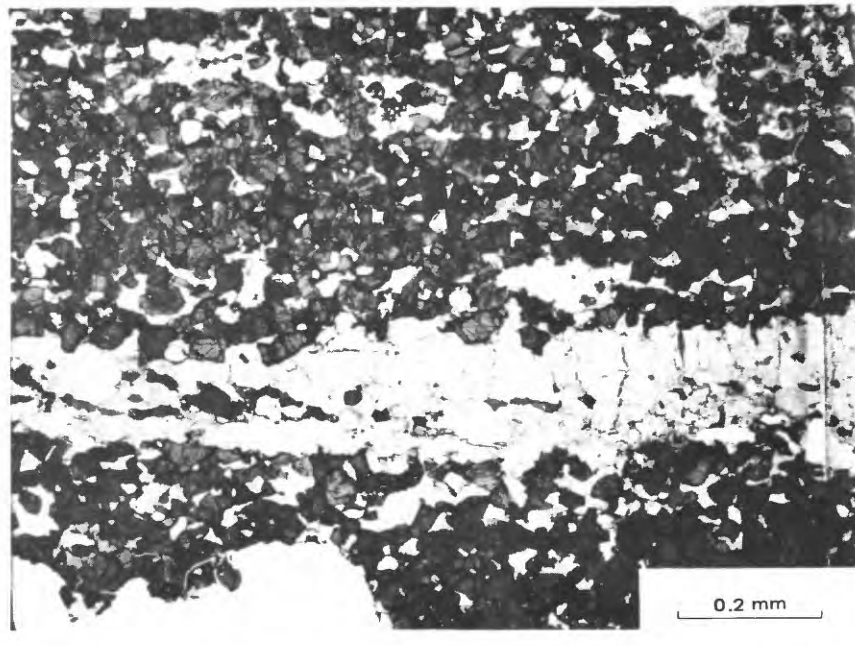

Figure 5. Photomicrograph of inclusion of layered gabbro showing alternating layers predominantly plagioclase and clinopyroxene, which have a cumulate fabric.

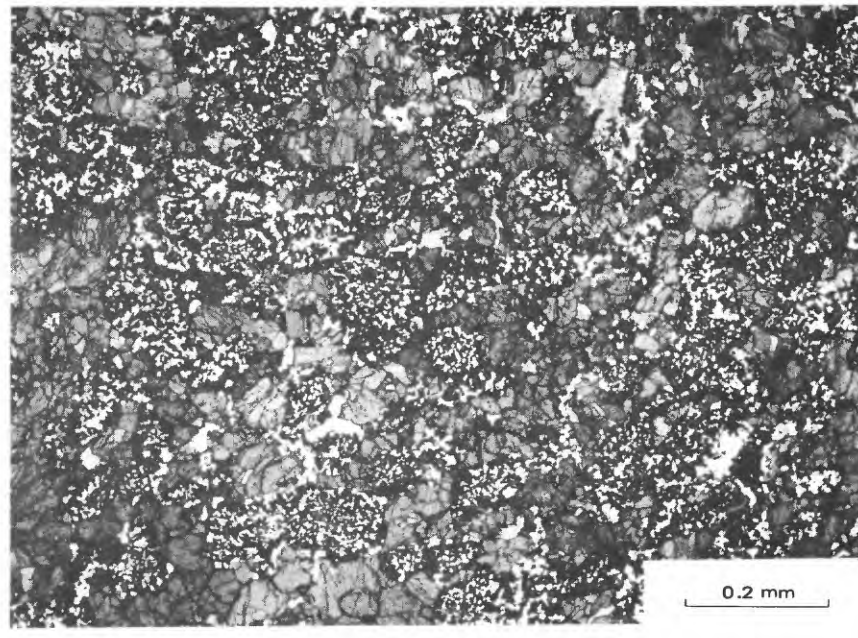

Figure 6. Photomicrograph of plagioclase websterite showing "reaction texture" composed of plagioclase, orthopyroxene, and chemically zoned spinel. Minor clinopyroxene locally present in reaction fabric.

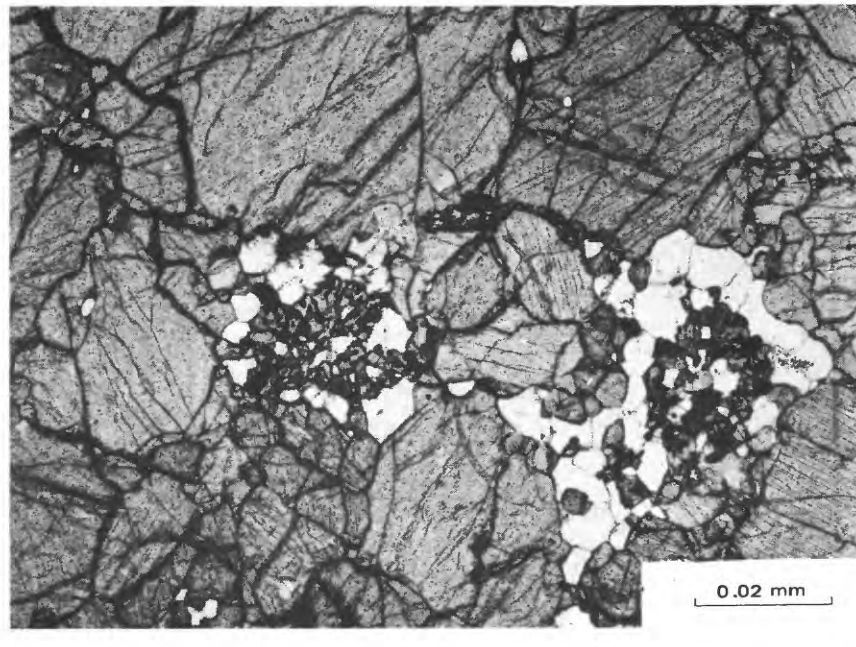

Figure 7. Photomicrograph of plagioclase websterite inclusion showing detail of "reaction texture" composed of plagioclase, orthopyroxene, and spinel in contact with clinopyroxene.

Gabbroic inclusions

Petrography

Inclusions collectively referred to as "gabbroic" range in grain size from fine to coarse grained (<1 to more than 5 mm) and in composition from plagioclase-clinopyroxenite and websterite through clinopyroxene-orthopyroxene gabbro to anorthositic gabbro. This range in composition can be seen in a single hand specimen, for example, sample 93427, where minerals of different composition define layers with cumulate texture (fig. 5), predominantly plagioclase and clinopyroxene.

In the more mafic layers, cumulus clinopyroxene is the dominant phase, and this clinopyroxene contains inclusions of plagioclase, orthopyroxene, and opaque minerals. Plagioclase also occurs as a cumulus phase, locally showing postcumulus crystallization between larger crystals of clinopyroxene. Orthopyroxene is less abundant as a cumulus phase but is more abundant in the "reaction texture" described below.

In the anorthositic gabbros, cumulus plagioclase showing postcumulus overgrowths contains inclusions of granular clinopyroxene and spinel. The plagioclase shows weak compositional zoning. "Reaction texture" is rare in anorthositic gabbro.

The "reaction texture" consists of domains or irregularly shaped areas, 4 mm or more in maximum dimension, composed of a mosaic of granular orthopyroxene and plagioclase (fig. 6, 7 and compare Nielson-Pike and Schwarzman, 1977, p. 52). Granular to elongate spinel is typically associated with the orthopyroxene, and small amounts of granular clinopyroxene locally occur within the "reaction texture". The "reaction texture" appears to corrode or marginally replace cumulus clinopyroxene. In some places, elongate spinel grains are partly enclosed in cumulus clinopyroxene and partly project into the "reaction texture". The cumulus clinopyroxene shows a consistent chemical zoning from cores of crystals toward rims adjacent to "reaction texture". (See discussion in section on Mineralogy). "Reaction texture" does not commonly show replacement relation with cumulus plagioclase. A typical mode of the "reaction texture" is 40 percent pyroxene, 40 percent spinel, and 20 percent plagioclase.

Textural relations within the "reaction fabric" and between the "reaction texture" and cumulus clinopyroxene suggest to us late-stage, relatively rapid crystallization from a melt. The composition of this melt is difficult to estimate because the "reaction texture" locally contains cumulus grains, and the composition of the spinels is extremely variable. It is clear that the "reaction texture"

of this mineralogy cannot be produced by simple partial melting of clinopyroxene and its subsequent recrystallization. The reaction assemblage is envisaged to have been derived largely from cumulus clinopyroxene with contributions from other cumulus phases and components from the enclosing basaltic lava. Possibly the melting was caused by decrease in pressure at high temperature as the gabbroic inclusions were being carried toward the surface by a rising alkalic basaltic magma.

Chemical analyses of three gabbroic inclusions presented in table 8 show all samples to be hypersthene-normative and one to be quartz-normative. These normative values and the trace-element analyses (table 8) reflect the high modal amounts of aluminous clinopyroxene, orthopyroxene, plagioclase, and spinel.

These gabbroic inclusions can be compared to those at Kod Ali Island (Hutchison and Gass, 1971), also thought to be of cumulate origin. Plagioclase from the Kod Ali inclusions is more calcic; they contain olivine and clinopyroxene in inclusions from the Wadi Hali locality. These mineralogical characteristics suggest to us that the gabbro inclusions from the Wadi Hali cone crystallized under higher pressure conditions than those from Kod Ali Island. Both sets of inclusions are encased in alkali olivine basalts, although those from Kod Ali are said to show a tholeiitic character (Hutchison and Gass, 1971).

Mineralogy

Plagioclase occurs both as a cumulate and an intercumulus phase (fig. 5) and in granoblastic aggregates with orthopyroxene and spinel ("reaction texture," figs. 6, 7). Cumulate plagioclase is compositionally zoned (An_{51-60}, $Or_{0.9-1.1}$), but with no consistent pattern (table 10). Granoblastic plagioclase is relatively homogeneous and is similar in composition to coexisting cumulus plagioclase (table 10).

Gabbroic inclusions contain both clinopyroxene and orthopyroxene. Both pyroxenes are chemically zoned in a consistent fashion. Large clinopyroxene crystals show an increase in aluminum and a decrease in silica from cores to rims (table 9, fig. 5). There is no change in Mg/Fe ratio. Cores of large orthopyroxene crystals are typically slightly lower in aluminum and higher in silicon than rims of the same crystals. Granular orthopyroxene in the "reaction texture" has a composition similar to that of rims of larger orthopyroxene crystals (table 11, fig. 5).

Spinel occurs in the "reaction texture" as equant to elongate grains, typically to 0.2 mm in length (figs. 6, 7). The spinels are predominantly magnesium-iron-aluminum spinels

and show extremely strong chemical zoning both within grains and from grain to grain. The observed range of molecular MgO/FeO is 0.420 to 2.473. The range in Al_2O_3 content is 43.5 to 69 weight percent, and TiO_2 and Cr_2O_3 generally make up less than 1 weight percent each. These compositions overlap those of spinel megacrysts and those present in websterites (table 5).

Other opaque phases include a few grains of ilmenite, which typically are 0.4 mm or greater in diameter and are not part of the "reaction texture" but appear to be postcumulus.

MEGACRYSTS

Clinopyroxene megacrysts

Large (about 2 cm) crystals of clinopyroxene associated with plagioclase and spinel megacrysts were studied from Jabal Haylah (sample 58377M) and the Wadi Hali (sample 98398) locality within the northern volcanics. The clinopyroxene megacrysts typically are black and glassy in appearance and have well-developed crystal faces (compare Irving, 1974c, p. 1503-1504). Because of the association of clinopyroxene megacrysts with clinopyroxenite and websterite inclusions at Jabal Haylah, it is tempting to relate the origin of the clinopyroxene megacrysts to that of the inclusions. Some of the megacrysts (for example, sample 58377M, table 6) have TiO_2, Al_2O_3, FeO total, and Na_2O contents comparable to that of clinopyroxene from the clinopyroxenite-websterite inclusions (tables 6, 7). The Cr_2O_3 content of 58377M, however, is significantly higher, and the megacryst contains chromite inclusions about 20 x 50 μm in size.

Clinopyroxene megacrysts from the Wadi Hali cone (98398 aM and bM, tables 6, 7) are much richer in Al_2O_3, TiO_2, and FeO total than clinopyroxenes of the ultramafic inclusions and are much closer to clinopyroxenes in the gabbroic inclusions (table 9). The clinopyroxenes of the gabbroic inclusions, however, show strong chemical zoning. Clinopyroxene megacrysts from the cone contain Mg-Fe-Al spinel inclusions approximately 100 μm in maximum dimension and oriented orthopyroxene inclusions about 50 μm in size.

The chemical homogeneity, common reaction rims with lavas, and similarity to liquidus clinopyroxenes experimentally observed to precipitate from alkali basalt liquids at high pressure (Green and Hibberson, 1970a; Green and Ringwood, 1967a) have led various workers to conclude that aluminous clinopyroxene megacrysts are high-pressure phenocrysts in basaltic magma (for example, Bacon and Carmichael, 1973). We favor this interpretation for the Jabal Haylah

and Wadi Hali clinopyroxene megacrysts, but the chemical differences between the clinopyroxenes of the two localities suggest precipitation under different physical and chemical conditions.

Plagioclase megacrysts

Plagioclase megacrysts to 1 cm in size are associated with clinopyroxene megacrysts from the Wadi Hali cone. The plagioclase megacrysts are largely unzoned with core compositions of $An_{43-45}Or_{2-2.8}$ (samples 93398, 93415). Near the margins of the megacrysts, an irregular zone of dusty inclusions separates the chemically homogeneous core from an outer chemically inhomogeneous zone of composition $An_{50-71}Or_{1-3}$. Microphenocrysts of plagioclase in the basalt adjacent to the megacrysts have compositions of $An_{50-71}Or_{1-3}$, which is comparable to the outer zone of the plagioclase megacrysts.

Some workers have interpreted andesine megacrysts to be higher-pressure phenocrysts, since groundmass plagioclase in basaltic lavas is generally more calcic, and experimental studies indicate that plagioclase crystallizing is more sodic with increasing pressure (Lindsley, 1968). The low An content of the Saudi Arabian plagioclase megacrysts therefore suggests that they also have formed at higher pressure than the groundmass plagioclase in the host basalt.

Spinel megacrysts

Spinel megacrysts are associated with plagioclase and clinopyroxene megacrysts from the Wadi Hali cone, but they tend to be far less abundant than the other species. The spinel megacrysts show little chemical zoning and have a lower chromium content and a higher Fe/Mg ratio and TiO_2 content than spinels from ultramafic inclusions (table 4). Some of the chemically zoned spinels from the "reaction texture" in the gabbro inclusions have Fe/Mg ratios comparable to those of the spinel megacrysts.

ALKALI OLIVINE BASALTS

Petrography and chemistry

The Al Birk basalt in the southern volcanic field, which rests on Miocene oceanic crust, is gray, fine grained, and vesicular, and contains phenocrysts of olivine set in an intergranular groundmass of plagioclase laths, pinkish clinopyroxene, olivine, and iron-titanium oxides. Several flows also contain groundmass nepheline, analcite, and chabazite. Phenocrysts of olivine (to 0.8 mm) are subhedral

and have iron-rich margins that are typically oxidized. Several samples of the basalt, for example, JT-26, contain xenocrysts of olivine derived by disaggregation of harzburgite inclusions. Olivine xenocrysts exhibit resorption and kink bands indicating disequilibrium with the basaltic magma and an earlier history of deformation. The lavas at Jabal Haylah in the northern volcanic field differ from those in the southern volcanic field in that they contain more clinopyroxene xenocrysts than olivine xenocrysts.

Comparison of averages for unpublished analyses of 46 samples of basalt from the northern volcanic field (unpublished data, 1976), with eight analyses of basalts from the southern volcanic field, shows no major differences between the two alkali olivine basalt suites. Four selected analyses, one from Jabal Akwah (JT-26) of the southern volcanic field containing harzburgite inclusions and three from Jabal Haylah (samples 58375, 58377, 58378) of the northern volcanic field containing websterite inclusions are presented in table 12. The basalts from Jabal Haylah are undersaturated, with nepheline present in samples 58375, 58377, 58378, and can be classified as basanites. Most lavas of the southern volcanic field are of either alkali olivine basalt or hawaiite; JT-26 is an alkali picrite rich in olivine with hypersthene in the norm and contains no nepheline. The host basalt for the inclusions at Jabal Akwah (JT-26) thereby appears to be more primitive than the average for all the Al Birk basalt. At least part of the unusual composition of JT-26 can be explained by contamination of xenocrystic olivine and orthopyroxene from disaggregated harzburgite inclusions.

Mineralogy

Olivine occurs as phenocrysts and xenocrysts and in the groundmass of alkali olivine basalts. Some of the olivines occur adjacent to harzburgite inclusions and are clearly crystals derived from the inclusions. Some of the olivine crystals contain strain bands similar to bands observed in olivine in harzburgite inclusions. Cores of large olivines have compositions near those of the olivines from harzburgite inclusions ($\sim Fo_{90}$, table 3), and their rims have compositions near those of groundmass olivines ($\sim Fo_{80}$, table 3). We infer that xenocrysts of olivine ($\sim Fo_{90}$) reacted with basaltic magma and developed rims with a composition near that in equilibrium with the magma. These rims are inferred to have developed after the basaltic magma and inclusions had moved up in the earth from the source of the inclusions. Olivine phenocrysts contain inclusions of chromite as much as 50 μm in size, whereas chromite inclusions of this size have not been observed in olivine from the harzburgites.

Plagioclase in the groundmass of the alkali olivine basalts is typically zoned (table 10) and has an average

composition near An_{60-65}. Microlites of plagioclase are commonly rimed by alkali feldspar (composition near $Or_{60}Ab_{28}An_{12}$). X-ray diffraction studies of mineral separates lighter than bromoform indicate that groundmass nepheline is a common constituent of these basalts. No reliable electron microprobe analyses of these nephelines were obtained.

Estimated quenching temperatures of basaltic lavas

Because of the scarcity of coexisting iron-titanium oxides in the Al Birk basalt, it was not possible to use the iron-titanium oxides geothermometer. A clinopyroxene-olivine geothermometer has been suggested by Powell and Powell (1974). (For a discussion of the validity of this geothermometer, see Wood, 1976). Application of the geothermometer to basalt 58377 (tables 3, 6) yields a temperature of 980°C. This is comparable to previously estimated temperatures on coexisting iron-titanium oxides from other alkali olivine basalts (see for example, Bacon and Carmichael, 1973, p. 7).

PRESSURE AND TEMPERATURE ESTIMATES

P-T equilibration of basaltic magma with mantle mineral assemblages

Alkali basalt magmas from the coastal plain of the Red Sea, Saudi Arabia, are inferred to have been derived by partial melting of the upper mantle at deeper levels in the mantle than those required for contemporaneous production of oceanic subalkaline basalts in the Red Sea axial trough (Coleman and others, 1977).

Nicholls and his coworkers (Nicholls and others, 1971; Nicholls and Carmichael, 1972; Carmichael and others, 1977) have presented methods by which one can estimate possible temperatures of equilibration of various magma types with mantle mineral assemblages. The theoretical background to the method and the necessary data are presented in these papers and will not be repeated here. Estimates of silica activity ($a SiO_2$) and alumina activity ($a Al_2O_3$) are made at the estimated quenching temperature of the basalt at the surface. Assuming that magma of the same composition existed at depth, expressions for the variation in $a SiO_2$ and $a Al_2O_3$ as a function of P and T are derived. These expressions are equated to similar expressions for $a SiO_2$ and $a Al_2O_3$ for mantle mineral assemblages, for example, $Mg_2SiO_4 + SiO_2 = 2MgSiO_3$ and $Mg_2SiO_4 + Al_2O_3 = MgAl_2O_4 + MgSiO_3$. Carmichael and others (1977, p. 397) use the following compositions and component activities for the mantle solid residue to calculate the equilibration

conditions of basic lavas: olivine (X Mg_2SiO_4 = 0.90), orthopyroxene (a $MgSiO_3$ = 0.73), and spinel (a $MgAl_2O_4$ = 0.614). Except for chromium-rich spinel, these activity-composition relations are very similar to those of the Saudi Arabian spinel harzburgites (JT-26B). Using a quenching temperature of 980°C, a silica activity defined by nepheline-albite, and an alumina activity defined by clinopyroxene-plagioclase suggests that alkali basalt magma similar to 58377 could have been in equilibrium with olivine-orthopyroxene-spinel, using mineral compositions from JT-26B, at a temperature near 1250°C and a pressure near 19 kbar (compare Bacon and Carmichael, 1973).

Mafic and ultramafic inclusions

Element partitioning between coexisting minerals in ultramafic inclusions has been used to estimate P-T conditions of equilibration in the inclusions (O'Hara, 1967; Boyd, 1973; Wood and Banno, 1973, and many other sources). For inclusions with complex histories, various geothermometers and geobarometers may be "frozen in" at varying pressures and temperatures. Wilshire and Jackson (1975) have pointed out some of the problems involved in the estimation of P-T conditions of equilibration in ultramafic inclusions.

Geothermometery based upon clinopyroxene-orthopyroxene equilibria is the subject of a voluminous literature. For recent reviews of the subject, see Evans (1977) and Herzberg (1978).

Wood and Banno (1973) developed a two-pyroxene geothermometer based on empirical corrections for the effects of elements other than CaO, MgO, and SiO_2 and neglected the effect of pressure on the estimation of temperature. Wells (1977) used additional experimental data and presented a revised version of the Wood-Banno geothermometer. Temperatures estimated from this geothermometer are presented in table 12.

Mori (1977) presented a calibration of the two-pyroxene geothermometer based on new experiments on subsolidus phase equilibria in the CaO-MgO-Al_2O_3-SiO_2 system and a natural spinel lherzolite. His calibration refers to a total pressure of 16 Kbar. Temperatures estimated from the Mori geothermometer are presented in table 12.

Herzberg (1978) considered several activity models for pyroxenes and, using some of the data treated by Mori, presented a calibration of the two-pyroxene geothermometer including a pressure correction. Temperature estimates at 16 kbar for ultramafic inclusions and at 10 Kbar for mafic inclusions based on this geothermometer are presented in table 12.

Table 12.--*Estimated equilibration temperatures of clinopyroxene and orthopyroxene in Saudi Arabian ultramafic and mafic inclusions*

	Sample	Wells (1977) modification of Wood and Banno geothermometer Estimated T°C	Mori (1977) geothermometer Estimated T°C	Herzberg (1978) geothermometer Estimated T°C
1.	JT26A	960	1110	1140
2.	JT26B	1030	1215	1230
3.	58476A	925	1140	1160
4.	58376B	985	1250	1265
5.	58376C	1050	1315	1335
6.	98413A	1010	1325	1325
7.	98413A	1010	1315	1315
8.	98413B	1015	1320	1320
9.	98413B	1010	1320	1320
10.	98410	1030	1340	1345
11.	98410	1040	1355	1365

Temperatures calculated from Equation 5 in Wells (1977), from equation 16 in Mori (1977) at 16 Kbar from equation 31 of Herzberg (1978) at 16 Kbar (1-5) and 10 Kbar (6-11). Samples 1-5 ultramafic inclusions; samples 6-11 gabbro inclusions; 6, 8, 10 calculated from cores of clinopyroxene and orthopyroxene; 7, 9, 11 calculated for rims of clinopyroxene and orthopyroxene in "reaction texture".

Temperature estimates based on the Mori and Herzberg geothermometers are considerably higher than those based upon the Wells modified geothermometer (table 12). Mori (1977) reported a number of temperature estimates on spinel lherzolite nodules in which the results from his calibration were significantly higher than those estimated from the Wood and Banno geothermometer. The temperatures estimated for the spinel harzburgites using the Wells geothermometer are below the liquidus temperatures for alkali olivine basalt and basanite at mantle pressures and below the temperature estimated from silica and alumina activity calculations for magma-mantle equilibration (see previous section). These temperature estimates and the textures of the harzburgites suggest subsolidus crystallization rather than high-pressure crystallization in equilibrium with basaltic magma. If, however, the temperature estimates from the Mori and Herzberg geothermometers are used, a closer physical proximity of the depth of magma segregation and the depth of incorporation of the harzburgite nodules is suggested (see also Mori, 1977, p. 276).

In the past several years, pressures of equilibration have been estimated from the aluminum content of orthopyroxenes in spinel- or garnet-bearing assemblages (for example, MacGregor, 1974). Several workers, for example, Wood (1975) and Newton (1978), have presented alternative interpretations of aluminum (in enstatite) isopleths; at this time, the pressure-temperature significance of the aluminum (in enstatite) isopleths is not completely understood.

A lower limit on equilibration pressure for the harzburgite inclusions is based upon the coexistence of clinopyroxene-orthopyroxene-spinel-olivine and the lack of stable olivine-plagioclase (for example, Irving, 1974b). According to experimental work presented by Green and Hibberson (1970b, p. 218), plagioclase disappears from "pyrolite" compositions at 11 to 12 Kbar at 1200°C. The stable assemblages would presumably represent pressures greater than about 10 Kbar at 1000°C. If we accept the hypothesis that these harzburgite inclusions can only be derived from the upper mantle, then the minimum pressure of incorporation of these xenoliths would be approximately 5 Kbar (based on a crustal thickness of approximately 15 km).

An upper limit on equilibration pressure of the harzburgite inclusions can be estimated by the absence of garnet in the inclusions, but the P-T field boundary between spinel- and garnet-bearing assemblages is strongly dependent on chemical composition. At temperatures near 1000°C spinel-bearing assemblages give way to garnet-bearing assemblages in a garnet lherzolite bulk composition, near 18 Kbar (O'Hara and others, 1971). For "pyrolite", garnet develops at 21 Kbar and 1100°C and at 24 Kbar and 1300°C at the expense of spinel (Green and Ringwood, 1967b). A reasonable upper limit for the pressure of equilibration of the Saudi Arabian harzburgite inclusions would be on the order of 20 Kbar.

Gabbros

Pyroxene equilibration temperatures for gabbroic inclusions and "reaction textures" in the inclusions show a range of only 30°-50°C (table 12) and, considering the uncertainties involved, these differences are probably not statistically significant. Using the Wells geothermometer these temperatures are below the liquidus temperatures of basaltic magmas for moderate to high pressures. Temperatures estimated from the Mori and Herzberg geothermometers are consistent with magmatic temperatures. Cumulate textures and layering suggest magmatic crystallization and crystal settling and are consistent with these latter temperature estimates. The high temperatures estimated for the reaction textures" are also consistent with magmatic crystallization.

The "reaction texture" is suggestive of rapid crystallization from a melt and the chemical zoning in the clinopyroxene and the orthopyroxene is clearly related to the "reaction texture". The simplest interpretation is that the "reaction texture" and the chemical zoning are related to incorporation of the inclusions in basaltic magma and the subsequent pressure decrease accompanying the rise of the basaltic magma and inclusions. If the hypersthene-normative and quartz-normative gabbros are included in alkali basalt and basanite magma it is possible that low silica activity in the magma will favor the following reaction, $CaAl_2Si_2O_8 = CaAl_2SiO_6 + SiO_2$ and will increase the aluminum content of clinopyroxene (see, for example, Carmichael and others, 1974, p. 273-274).

Clinopyroxene and plagioclase megacrysts

Bacon and Carmichael (1973) and Carmichael and others (1977) have estimated the P and T of equilibration of clinopyroxene and plagioclase megacrysts with basanitic magma (samples from San Quintin, Mexico). In the earlier paper (1973) they estimated equilibration pressures of 9.2-10.6 Kbar and temperatures of 1045-1055°C. In the second paper they argued that the precipitation of the megacrysts represents a thermal response of the incorporation of cooler ultramafic nodules in hot basaltic magma. If this model is correct and ultramafic nodules come from the mantle, pressures of equilibration should be greater than 10-12 Kbar for continental basanites and at temperatures appropriate to the lava liquidus. Carmichael and others (1977, p. 390, 402) use different activity-composition models for jadeite and Ca-Tschermak's molecule in clinopyroxene and calculate equilibration pressures of 16-17.3 bar and temperatures of 1235°C. Applying this model to the Saudi Arabian megacrysts and lavas yields T >1350°C and P on the order of 16 Kbar. Green and Hibberson (1970a) were able to experimentally crystallize clinopyroxene megacrysts in alkali basalt liquid near 1200°C, P = 14-16 Kbar and with approximately 2 percent H_2O in the liquid. However, a sodium-rich feldspar was not recorded in these experiments and has not been crystallized in high pressure experiments near the liquidus (Green and Ringwood, 1967a; Irving, 1974c). The very common presence of essentially homogeneous plagioclase megacrysts in nodule-bearing alkali basalts is difficult to reconcile with the present experimental data. The field data from Saudi Arabia also seems difficult to reconcile with this model. Megacrysts are associated with pyroxene-rich inclusions and gabbroic inclusions and are not found in lavas that have erupted through a 15 km thick oceanic crust. These lavas, however, contain depleted spinel harzburgite inclusions. Gabbros and megacrysts, which clearly have crystallized from magma at depth, have been incorporated into lavas which have traversed a thick (48 km) continental crust. Gabbroic inclusions show cumulate textures and layering suggesting crystallization and accumulation in a magma that was not rapidly ascending.

Carmichael and others (1977) speculate, however, that because megacrysts are unzoned they precipitated and grew so quickly that their composition was unaffected by change of P and T during the upward movement of the enclosing magma.

CONCLUSIONS

Although the precise P-T conditions under which the inclusions formed are uncertain, the relative values of temperature, textures and structures of the inclusions and their geologic setting provide some insight into the evolution of the Al Birk basalt and its inclusions.

The aluminum-rich clinopyroxene, sodic plagioclase, and spinel megacrysts are inferred to be of cognate origin and to have crystallized from basaltic magma. The cumulus clinopyroxene of the websterite inclusions are thought to represent fractional crystallization from a basaltic magma. Based upon available experimental data, the plagioclase megacrysts formed at depths no greater than that of the lower crust, but the clinopyroxene megacrysts could have crystallized under upper mantle pressures. The fact that plagioclase (An_{51-60}, table 10) is a cumulus phase with clinopyroxene in the gabbroic inclusions implies that they crystallized under similar pressure conditions, possibly in the lower crust. The occurrence of cumulus textures and layering within these inclusions suggests that these phases crystallized when the magma was not rapidly ascending. These types of inclusions are restricted to areas underlain by thick (48 km) Precambrian crust. Chemical zoning within pyroxenes and the presence of "reaction texture" adjacent to the cumulus clinopyroxene suggests that a new reaction, including possible partial melting, may have occurred in response to pressure decrease accompanying rapid uprise of the inclusions within ascending basaltic magma.

In contrast, the inclusions from the oceanic crust section (15 km thick) consist of spinel harzburgite only. These harzburgites are present in the continental sector but are much less abundant than the cumulate xenoliths. The harzburgites do not exhibit a tectonite fabric as reported for similar occurrences (for example, Basu, 1975). The harzburgites are generally inferred to be composed of refractory and depleted mantle material from which a low-melting basaltic magma has been extracted and most workers believe that spinel harzburgite inclusions are accidental mantle fragments. If this is true, and the harzburgites are indeed refractory residues, then the host basalt magmas of the Al Birk basalt must have been derived from undepleted mantle at greater depth. Calculations of inferred pressures of equilibration of basaltic magma with mantle mineral assemblages suggests that the depleted harzburgite inclusions came from depths less than about 70 km (pressure less than 20-24 Kbar).

REFERENCES CITED

Albee, A.L., and Ray, L., 1970, Correction factors for electron probe microanalysis of silicates, oxides, carbonates, phosphates, and sulfates: Analytical Chemistry, v. 42, p. 1408-1414.

Bacon, C.R., and Carmichael, I.S.E., 1973, Stages in the P-T path of ascending magma--an example from San Quintin, Baja, California: Contributions to Mineralogy and Petrology, v. 4, p. 1-22.

Baker, B.H., Mohr, P.A., and Williams, L.A.J., 1972, Geology of the eastern rift system of Africa: Geological Society of America Special Paper 136, 67 p.

Basu, A.R., 1975, Hot-spots, mantle plumes, and a model for the origin of ultramafic xenoliths in alkali basalts: Earth and Planetary Science Letters, v. 28, p. 261-274.

Bence, A.E., and Albee, A.L., 1968, Empirical correction factors for the electron microanalysis of silicates and oxides: Journal of Geology, v. 76, p. 382-403.

Boyd, F.R., 1973, A pyroxene geotherm: Geochimica et Cosmochimica Acta, v. 37, p. 2533-2546.

Carmichael, I.S.E., Turner, F.J., and Verhoogen, Jean, 1974, Igneous petrology: New York, McGraw-Hill, p. 714.

Carmichael, I.S.E., Nicholls, J., Spera, F.J., Wood, B.J., and Nelson, S.A., 1977, High-temperature properties of silicate liquids: applications to the equilibration and ascent of basic magma: Philosophical Transactions of the Royal Society of London, A, v. 286, p. 373-431.

Coleman, R.G., Fleck, R.J., Hedge, C.E., and Ghent, E.D., 1977, The volcanic rocks of southwest Saudi Arabia and the opening of the Red Sea: Saudi Arabian Directorate General of Mineral Resources Bulletin 22-D, p. 1-30.

Evans, B.W., 1977, Metamorphism of alpine peridotite and serpentinite: Annual Review of Earth and Planetary Science, v. 5, p. 397-447.

Gettings, Mark, 1977, Delineation of the continental margin in the southern Red Sea from new gravity evidence: Saudi Arabian Directorate General of Mineral Resources Bulletin 22-K, p. 1-11.

Green, D.H., and Hibberson, W., 1970a, Experimental duplication of conditions of precipitation of high pressure phenocrysts in a basaltic magma: Physics of the Earth and Planetary Interiors, v. 3, p. 247-254.

Green, D.H., and Hibberson, W., 1970b, The instability of plagioclase in peridotite at high pressure: Lithos, v. 3, p. 209-221.

Green, D.H., and Ringwood, A.E., 1967a, The genesis of basaltic magmas: Contributions to Mineralogy and Petrology, v. 15, p. 103-190.

_____1967b, The stability fields of aluminous pyroxene peridotite and garnet peridotite and their relevance in upper mantle structure: Earth and Planetary Science Letters, v. 3, p. 151-160.

Hadley, D.G., 1975a, Geology of the Al Qunfudhah quadrangle, sheet 19/41C, Kingdom of Saudi Arabia: Saudi Arabian Directorate General of Mineral Resources Geologic Map GM-19, scale 1:100,000.

_____1975b, Geology of the Wadi Hali quadrangle, sheet 18/41B, Kingdom of Saudi Arabia: Saudi Arabian Directorate General of Mineral Resources Geologic Map GM-21, scale 1:100,000.

Herzberg, C.T., 1978, Pyroxene geothermometry and geobarometry: experimental and thermodynamic evaluation of some subsolidus phase relations involving pyroxenes in the system $CaO-MgO-Al_2O_3-SiO_2$: Geochemica et Cosmochimica Acta, v. 42, p. 945-957.

Hutchison, R., and Gass, I.G., 1971, Mafic and ultramafic xenoliths associated with undersaturated basalt on Kod Ali Island, southern Red Sea: Contributions to Mineralogy and Petrology, v. 31, p. 94-101.

Irving, A.J., 1974a, Pyroxene-rich ultramafic xenoliths in the Newer basalts of Victoria, Australia: Neues Jahrbuch Mineralogie Abhandlung, v. 120, p. 147-167.

_____1974b, Geochemical and high pressure experimental studies of garnet pyroxenite and pyroxene granulite xenoliths from the Delegate basaltic pipes, Australia: Journal of Petrology, v. 15, p. 1-40.

_____1974c, Megacrysts from the Newer basalts and other basaltic rocks of southeastern Australia: Geological Society of America Bulletin, v. 85, p. 1503-1514.

Lindsley, D.H., 1968, Melting relations of plagioclase at high pressures: New York State Museum and Science Memoirs, v. 18, p. 39-46.

MacGregor, I.D., 1974, The system $MgO-Al_2O_3-SiO_2$--solubility of Al_2O_3 in enstatite for spinel and garnet peridotite compositions: American Mineralogist, v. 59, p. 110-119.

Mori, T., 1977, Geothermometry of spinel lherzolites: Contributions to Mineralogy and Petrology, v. 59, p. 261-279.

Newton, R.C., 1978, Experimental determination of the spinel peridotite to garnet peridotite reaction in the system $MgO-Al_2O_3-SiO_2$ in the range 900°-1100°C and Al_2O_3 isopleths of enstatite in the spinel field: Contributions to Mineralogy and petrology, v. 66, p. 189-201.

Nielson Pike, J.E., and Schwarzman, E.C., 1977, Classification of textures in ultramafic xenoliths: Journal of Geology, v. 85, p. 49-61.

Nicholls, J.W., Carmichael, I.S.E., and Stormer, J.C., Jr., 1971, Silica activity and P total in igneous rocks: Contributions to Mineralogy and Petrology, v. 33, p. 1-20.

Nicholls, J.W., and Carmichael, I.S.E., 1972, The equilibration temperature and pressure of various lava types with spinel and garnet peridotite: American Mineralogist, v. 57, p. 941-959.

O'Hara, M.H., 1967, Mineral facies in ultrabasic rocks, *in* Wyllie, P.J., ed., Ultramafic and related rocks: New York, John Wiley and Sons, p. 7-18.

O'Hara, M.H., Richardson, S.W., and Wilson, G., 1971, Garnet peridotite stability and occurrence in crust and mantle: Contributions to Mineralogy and Petrology, v. 32, p. 48-68.

Powell, M., and Powell, R., 1974, An olivine-clinopyroxene geothermometer: Contributions to Mineralogy and Petrology, v. 48, p. 249-263.

Ross, C.S., Foster, M.D., and Myers, A.T., 1954, Origin of dunites and of olivine-rich inclusions in basaltic rocks: American Mineralogist, v. 39, p. 693-737.

Ross, D.A., Whitmarsh, R.B., Ali, S.A., Boudreaux, J.D., Coleman, R., Fleisher, R.L., Girdler, R., Manheim, F., Matter, A., Nigrini, C., Stoffers, P., and Supko, P.R., 1973, Red Sea drillings: Science, v. 179, p. 377-380.

Talbot, J.L., Hobbs, B.E., Wilshire, H.G., and Sweatman, T.R., 1963, Xenoliths and xenocrysts from lavas of the Kerguelen Archipelago: American Mineralogist, v. 48, p. 159-179.

Wells, P.R.A., 1977, Pyroxene thermometry in simple and complex systems: Contributions to Mineralogy and Petrology, v. 62, p. 129-139.

White, R.W., 1966, Ultramafic inclusions in basaltic rocks from Hawaii: Contributions to Mineralogy and Petrology, v. 12, p. 245-314.

Wilshire, H.G., and Jackson, E.D., 1975, Problems in determining mantle geotherms from pyroxene compositions of ultramafic rocks: Journal of Geology, v. 83, p. 313-329.

Wood, B.J., 1975, The application of thermodynamics to some sub-solidus equilibria involving solid solutions: Fortschritte Mineralogie, v. 52, p. 21-45.

_____1976, An olivine-clinopyroxene geothermometer, a discussion: Contributions to Mineralogy and Petrology, v. 56, p. 297-304.

Wood, B.J., and Banno, S., 1973, Garnet-orthopyroxene and orthopyroxene-clinopyroxene relationships in simple and complex systems: Contributions to Mineralogy and Petrology, v. 42, p. 109-124.

APPENDIX

Electron microprobe analytical techniques

Most of the mineral analyses reported in this paper were obtained by an ARL-EMX electron probe microanalyzer. Operating conditions were: accelerating voltage, 15 kv; beam current, 0.5 to 1.0 microamps. Data were corrected according to methods outlined by Bence and Albee (1968) and Albee and Ray (1970). An estimate of the accuracy of the electron microprobe analyses is presented in table 5, which gives analyses of spinel 93398A megacrysts by both electron microprobe and wet chemical techniques. The SiO_2 content of spinel is likely to be near the microprobe values (0.03) and the SiO_2 reported in the wet chemical analysis is likely to be present in silicate impurities. This impurity will affect the other constituents in the analysis, but even disregarding the SiO_2 value, the agreement between the two analyses is reasonable.